Available online at www.sciencedirect.com
SCIENCE DIRECT®
ELSEVIER
Journal of Nuclear Materials 336 (2005) 140–144
journal of nuclear materials
www.elsevier.com/locate/jnucmat

# Determination of the helium thermal diffusion coefficient in britholite using a NRA method: new results

Dominique Gosset [a,*], Patrick Trocellier [b]

[a] *CEA Saclay bat. 453, DMN/SRMA/LA2M, Gif/Yvette F-91191, France*
[b] *CEA Saclay bat 520, DMN/SRMP, F-91191 Gif/Yvette, France*

Received 2 April 2004; accepted 31 August 2004

**Abstract**

Dimensioning of actinides waste packages for long duration storage has to take into account helium production from natural decay and release rates from the material. For the latter, we propose here an improved method for the determination of the helium diffusion coefficient in britholite, to be used for minor actinides storage. This work is based on results we previously published using the classical three steps method: $^3$He implantation on a Van de Graaff facility, $^3$He profile determination analysing the protons resulting from the $^3$He(d,**p**)$^4$He reaction in a nuclear microprobe, evolution of the helium profile during annealings. Taking explicitly into account the incident deuterons energy stragglings allows us to show that the implanted helium profiles are bimodal, each component leading to a different helium diffusion coefficient.


## 1. Introduction

α-decay of actinide isotopes will lead to high helium production rates in the inert matrices used for long duration storage. It is then of primary importance to evaluate the helium diffusion coefficients in these materials in the temperature range of a disposal area. In a previous paper, we detailed the results obtained by analysing the helium profiles resulting of ion implantation and subsequent annealings by a nuclear-reaction analysis, namely the $^3$He(d,p)$^4$ He reaction [1]. Two analysis methods were developed. The first one is the classical excitation curve method, consisting in the analysis of the $N_p(E_d)$ curve, i.e. the number of protons resulting of the (d,p) reaction as a function of the incident deuterons energy. The second one is based on an accurate description of the $N_p(E_p)$ curve, i.e. the number of protons as a function of their energy for a given incident deuterons energy. Both methods aim at reconstructing the helium profile from a given distribution of the collected protons, either their yield as a function of the incident deuteron energy or their energy distribution for a given incident deuteron energy. But in both cases, the effect of the energy dispersions (straggling of the incident deuterons as they slow down in the material and of the collected protons as they travel back to the detector) were considered only as an apparent broadening of the helium profiles. As a result, the diffusion coefficient we derived were obtained from differences of the resulting apparent profile widths before and after annealings

* Corresponding author. Tel.: +33 1 69 08 58 57; fax: +33 1 69 08 90 82.
*E-mail addresses:* dgosset@cea.fr (D. Gosset), patrick.trocellier@cea.fr (P. Trocellier).

0022-3115/$ - see front matter © 2004 Published by Elsevier B.V.
doi:10.1016/j.jnucmat.2004.08.012

and we were unable to have an accurate description of the actual helium distributions. We describe here some improvements we have performed which allow a better description of the actual helium profiles.

## 2. Experiment

The analysis were performed on high quality, nearly fully dense Nd-britholite samples with different grain sizes (Fig. 1), elaborated by calcinations of simple oxide powders and subsequent sintering [2]. The samples were cut and polished prior ion implantations. The $^{3}$He implantations were performed on a Van-de-Graaff accelerator at IPN Lyon (3 MeV, $2 \times 10^{16}$ ions/cm$^2$, homogeneity ± 10% in analysed areas). The samples were then cut, one part of each annealed for 35 mn at 400 °C to have a significant helium profile broadening.

The helium analysis were performed at LPS Laboratory in similar conditions as in [1]. In order to reduce the distortions of the proton energy curves we subsequently analysed, the energy of the incident deuteron beam was set at 1500 keV: in this case, the helium profile intersects the reaction yield curve on its high energy, rather flat, side (Fig. 2). The deuteron beam was around $50 \times 50\,\mu m^2$, its intensity was around 5 nA. The back-scattered deuterons were stopped with a 25 μm thick mylar® film, a low-$Z$ material that limits the proton energy straggling. For each sample, at least 10 analysis (deuteron fluence = 10 μC) were performed.

## 3. Data processing

With the excitation curve method, the protons yield is given (neglecting straggling) by the convolution of the helium concentration and the (d,p) reaction cross section:

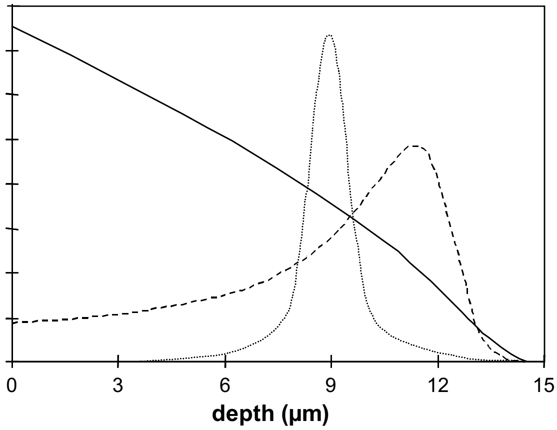


Fig. 2. Simulation of the $^{3}$He(d,p)$^{4}$He experiment (without stragglings): mean deuteron energy (full line), helium concentration (dotted line) and $^{3}$He(d,p)$^{4}$He reaction cross section (dashed line) versus depth. Scales: initial deuteron energy = 1500 keV, max. $^{3}$He concentration = 1.10$^{20}$ cm$^{-3}$, max. cross section = 64.7 mbarn/Sr.

$$N_p(E_d) = N_d(E_d) \int_{x=0}^{\infty} \frac{d\sigma(E_d(x))}{d\Omega} \rho(x) dx \qquad (1)$$

with $\rho(x)$ the $^{3}$He concentration at depth $x$, rm $d\sigma/d\Omega$ the differential cross-section of the $^{3}$He(d,p)$^{4}$He reaction calculated in the actual experimental configuration for a deuteron energy $E_d(x)$ given as:

$$E_d(x) = E_d - g(x),$$

the energy of the interacting deuterons at depth $x$, with:

$$g(x) = \int_0^x \frac{\partial E_d}{\partial u} du \qquad (2)$$

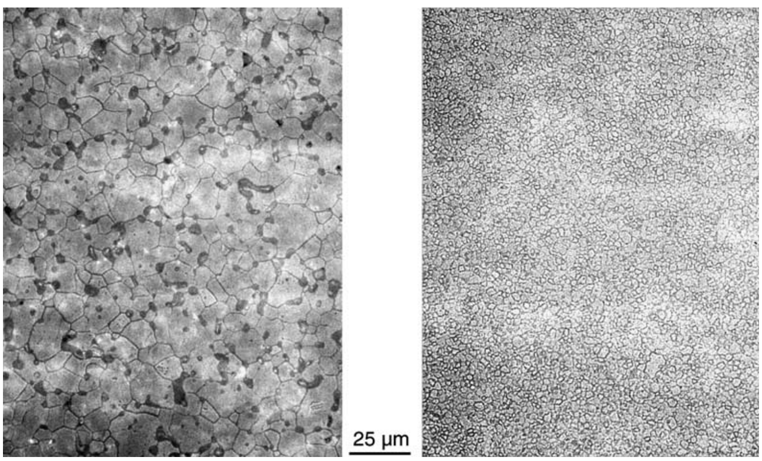


Fig. 1. Microstructure of the britholite samples (left: 31-4, mean grain size = 16 μm; right: 34-8, mean grain size = 2.6 μm).

the deuteron energy loss from the sample surface to the depth $x$; with $\partial E_d/\partial u$ the stopping power of the deuterons in the material.

$N_d$ the number of deuterons of initial energy $E_d$; $\Omega$ the solid angle of the proton detector.

This method leads to a coarse determination of the helium profile, the resolution being limited by the shape of the $d\sigma/d\Omega$ curve.

On the other hand, analysing the proton energy curve leads to a more straightforward determination of the helium profile:

$$\frac{dN_p}{dE_p}(E_p) = N_d(E_d)\Omega\frac{d\sigma(E_d - g(x))}{d\Omega}\rho(x)dx, \qquad (3)$$

where $E_d$ can be chosen in order to obtain a nearly flat $d\sigma/d\Omega$ curve in the zone of interest, i.e. the helium profile: in this case, $dN_p/dE_p(E_p)$ can be considered just as a slightly distorted energy image of the $\rho(x)$ profile.

Moreover, this second approach allows taking into account the stragglings. The following method was used here: on a first step, $\overline{E_d(x)}$, the mean deuteron energy at depth $x$, is determined from Eq. (2) using the same approximations as in [1]. It is then possible to determine the corresponding values of the following parameters versus depth: $d\sigma/d\Omega$, $E_p(x)$. It is also possible to derive an estimation of the deuteron energy straggling, using the Bohr formula and/or Tschälar approximation [3]. Moreover, since protons are detected on a multi-channel detector with constant energy width channels, it is interesting to convert the $x$ depth scale in $\overline{E_p(x)}$ proton energy scale, with $\overline{E_p(x)}$ the mean proton energy emitted at depth $x$; this is made possible using the kinematics of the (d,p) reaction provided the corresponding proton yield is corrected for the $dE_p/dx$ factor.

The energy straggling of the protons as they travel back through the sample can also be evaluated and added (quadratic sum) to the previous one to obtain an apparent total proton straggling. In the energy losses range we consider here, this resultant straggling can be considered as the variance of a normal proton energy distribution [3]. We then make the hypothesis that the protons created at a depth $x$, i.e. at a mean energy $\overline{E_p(x)}$ are distributed according a normal function which variance $S(\overline{E_p})$ is the total apparent proton straggling. The number of protons collected for a given proton energy (channel of the detector) is then given by the convolution product:

$$N_p(\overline{E_p}) = \int_{-\Delta E}^{+\Delta E} N_p(\overline{E_p} - E_p)G(E_p)dE_p \qquad (4)$$

with $G(E_p)$ the normal function which variance is the total straggling $S(\overline{E_p})$ and the integration can be for practical use limited to $\pm\Delta E = 3S(\overline{E_p})$.

## 4. Results

We have first checked the method by analysing all the individual proton energy curves obtained when performing an excitation curve analysis. We have used the set of curves obtained in [1] in the case of a non-annealed Nd-britholite. The following results were obtained (Fig. 3):

- the whole set of curves can be fitted using a single set of experimental parameters, even the low-deuteron energy curves for which the deuterons are stopped before and partly inside the helium profile: this is of primary importance since in this case, only the low-depth side of the helium profile is analysed, leading to highly distorted proton energy curves;
- using a full set of curves (here, 8 curves for $E_d$ ranging from 1700 keV to 1150 keV) allows an estimation of the actual mean depth of the helium profile. The value we determine here is somewhat lower than SRIM estimation (8.95 μm vs 9.03 μm), but much closer than the value derived from the excitation curve method (8.64 μm: [1]). Thanks to the low-deuteron energy effect we detailed just above, this depth value is here determined with a very high sensitivity, around ± 0.02 μm;
- the best results are obtained assuming deuteron straggling values intermediate of Bohr and Tschälar approximations;
- assuming a normal distribution for the helium profile leads to a variance quite close to SRIM straggling estimation (0.15 μm vs 0.13 μm). But, due to the stragglings (mainly the deuterons one), this value

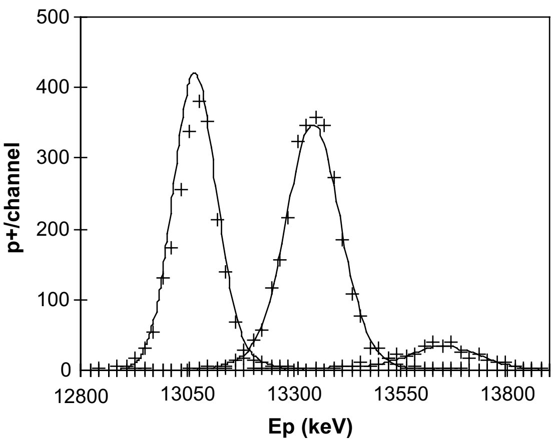


Fig. 3. Simulation of the proton energy curves for selected incident deuterons energies (from left to right, 1400 keV, 1250 keV, 1150 keV). It should be noticed that in the 1150 keV case, the deuterons are totally stopped before and inside the helium profile, leading to large distortions of the corresponding proton energy curve which could not be accounted neglecting stragglings effects.

appears to be the resolution limit of the method (for an implantation depth around 9 μm);

- in order to fit the tails of the proton energy curves, we are lead to assume that the helium profile has larger tails than the normal (SRIM) distribution: a second, wider (variance = 0.65 μm), minor (15% of total helium) gaussian component was then added to the main one.

We have then analysed the new Nd-britholite samples. The results are summarized on Table 1:

- as in the previous analysis, it is necessary to assume a bi-modal helium profile. This was checked with a SIMNRA analysis [4] which shows that using a profile as narrow as a gaussian function could not lead to a correct fitting of the tails of the proton energy distributions;
- since only one deuteron energy is used, it is not possible to derive the mean depth of the profile: we have then considered the value estimated by SRIM (9.03 μm). The energy position of the profile has then to be adjusted via the energy width of the detector channels;
- before annealing, the second component appears narrower ($\sigma$ = 0.80 μm vs 1.5 μm) and more important (40% vs 35%) for the low grain size sample (34-8, 2.6 μm). The depth difference (< 0.1 μm) is not here significant. After annealing, the broad components have nearly the same characteristics.

Table 1
Helium profile analysis for the as-implanted and annealed Nd-britholite samples (34–38 non annealed: 2 samples)

| | Non annealed | | Ann. 400 °C | |
|---|---|---|---|---|
| *31-4* | keV/ch.: 14.636 | | keV/ch.: 14.641 | |
| (gr. size 16 μm) | G1 | G2 | G1 | G2 |
| Depth (μm) | 9.03 | 9.05 | 9.03 | 9.07 |
| $\sigma$ (μm) | 0.15 | 1.5 | 0.45 | 1.80 |
| FWHM (μm) | 0.35 | 3.45 | 1.06 | 4.03 |
| Fraction | 0.67 | 0.33 | 0.63 | 0.37 |
| $^{3}$He/cm$^{2}$ × 10$^{16}$ | 1.039 | 0.511 | 0.99 | 0.58 |
| $^{3}$He total | 1.55 | | 1.57 | |
| $^{3}$He$_{max}$/cm$^{3}$/10$^{20}$ | 2.898 | | 1.02 | |
| *34-8* | keV/ch.: 14.637 | | keV/ch.: 14.638 | |
| (gr. size 2.6 μm) | G1 | G2 | G1 | G2 |
| Depth (μm) | 9.03 | 8.95 | 9.03 | 9.00 |
| $\sigma$ (μm) | 0.12 | 0.8 | 0.50 | 1.80 |
| FWHM (μm) | 0.28 | 1.84 | 1.18 | 4.18 |
| Fraction | 0.6 | 0.4 | 0.65 | 0.35 |
| $^{3}$He/cm$^{2}$ × 10$^{16}$ | 0.9 | 0.6 | 1.01 | 0.54 |
| $^{3}$He total | 1.50 | | 1.55 | |
| $^{3}$He$_{max}$/cm$^{3}$/10$^{20}$ | 3.29 | | 0.98 | |

keV/ch.: energy width of proton detector channels; G1, G2: main (narrow) and secondary (broad) contributions to helium profiles; $\sigma$ and FWHM: variance and full-width at half maximum of the profile components.

Table 2
Thermal diffusion coefficients of helium in Nd-britholite at 400 °C

| Component | Narrow | | Broad | |
|---|---|---|---|---|
| | 31-4 | 34-8 | 31-4 | 34-8 |
| gr. size (μm) | 16 | 2.6 | 16 | 2.6 |
| 1000/T (K$^{-1}$) | 1.4859 | 1.4859 | 1.4859 | 1.4859 |
| $D$(cm$^{2}$/s)*10$^{13}$ | 4.091 | 4.258 | 16.75 | 49.95 |
| log$_{10}$$D$ | −12.39 | −12.37 | −11.78 | −11.30 |

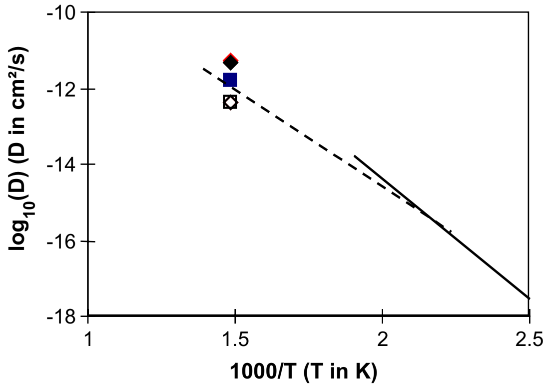


Fig. 4. Helium diffusion coefficient in Nd-britholite; diamond: low grain size; square: large grain size; open symbols: narrow component; full symbols: broad component; dashed line: [1]; full line: from [5] (natural apatites); errors: $\log_{10}D \pm 0.2$.

From the helium profile broadenings, it is then possible to derive thermal diffusion coefficients. The values we obtain for the narrow and the broad components (Table 2, corrected for the $^{3}$He/$^{4}$He atomic mass ratio) are significantly different. They enclose the values we obtained in [1] (Fig. 4). The two components could be attributed either to different intra- and inter-granular helium diffusion coefficients or to anisotropic intragranular diffusion (e.g. along the (0 0 1) channels of the hexagonal structure). It can be deduced that in the temperature conditions of a deep depository area, the helium release rate would be higher than the production resulting from $\alpha$-decay.

## 5. Conclusion

We propose here an improved analysis of the proton energy curves obtained from the well-known $^{3}$He(d,p)$^{4}$He NRA method. Taking explicitly into account the incident deuterons and detected protons stragglings allows a better description of the $^{3}$He distribution in the analysed material. In the case of Nd-britholite, we deduce that the helium profiles are bi-modal. The thermal diffusion coefficients we derive are in agreement with previous determinations: in the temperature conditions of a repository area, high release rates are to be expected.

## Acknowledgments

We are very indebted in F.Audubert (CEA-Cadarache, DED/SEP/LEMC) who elaborated the materials and A. Chevarier and A. Gardon (IPN, Lyon) who performed the $^{3}He$ implantations.

## References

[1] D. Gosset, P. Trocellier, Y. Serruys, J. Nucl. Mater. 303 (2002) 115.
[2] F. Audubert, private communication.
[3] J. Tirira, Y. Serruys, P. Trocellier, Forward Recoil Spectrometry, Plenum, 1996.
[4] M. Mayer, SIMNRA, http://www.physics.isu.edu/sigmabase/programs/simnra44.html.
[5] S. Ouchani, J.C. Dran, J. Chaumont, Appl. Geochem. 13–16 (1998) 707.